# Fabrication of *para*-dimethylamine calix[4]arene functionalized self-assembled graphene oxide composite material for effective removal of 2, 4, 6-tri-Cholorphenol from aqueous environment

Ali Hyder [a], Muzamil Thebo [b], Dahar Janwery [a], Jamil Ahmed Buledi [a], Imamdin Chandio [c], Awais Khalid [d,**], Bader S. Al-Anzi [e], Hanadi A. Almukhlifi [f], Khalid Hussain Thebo [g], Fakhar N. Memon [h], Ayaz Ali Memon [a,*], Amber Rehana Solangi [a], Shahabuddin Memon [a]

[a] *National Centre of Excellence in Analytical Chemistry, University of Sindh, Jamshoro, 76080, Pakistan*
[b] *Dr. M. A. Kazi Institute of Chemistry, University of Sindh, Jamshoro, 76080, Pakistan*
[c] *Department of Chemistry Tsinghua University, Beijing, 100084, China*
[d] *Department of Physics, Hazara University Mansehra, Mansehra, Khyber Pakhtunkhwa, 21300, Pakistan*
[e] *Department of Environment Technologies and Management, Kuwait University, P.O. Box 5969, Safat, 13060, Kuwait*
[f] *Department of Chemistry, Faculty of Science, University of Tabuk, Tabuk, 71491, Saudi Arabia*
[g] *Institute of Metal Research (IMR), Chinese Academy of Science, 2 Wenhua Rood, Shenyang, China*
[h] *Department of Chemistry, University of Karachi, Sindh, Pakistan*

## A R T I C L E  I N F O

## A B S T R A C T

Water pollution caused by the release of organic pollutants is a major environmental concern worldwide. These pollutants can have harmful effects on aquatic ecosystems and the organisms living within them, as well as on human health when contaminated water is consumed. It is essential to implement proper treatment and management strategies to prevent and mitigate water pollution. Moreover, the major untreated industrial effluents are synthetic organic compounds especially 2,4,6-trichlorophenol (TCP) which cause several environmental issues and heath related problems in humans. To cope with this problem, an excellent 2D porous material based on *p*-DMAC4/GO composite has been synthesized as adsorbent material for the effective removal of 2,4,6-trichlorophenol pollutant from wastewater. In this regard, the advanced analytical tools such as Fourier-Transform infrared (FT-IR), X-ray Diffraction (XRD), Scanning Electron Microscopy (SEM) and Energy-Dispersive X-ray spectroscopy (EDS) were used for its characterization. The results justified the chemical composition, excellent crystalline nature, surface morphology and elemental composition of the synthesized composite material. The synthesized adsorbent material showed 95% adsorption of TCP from wastewater system at optimal conditions *i.e.,* pH (6), adsorbent dosage (30 mg) and shaking time (60 min). The mathematical models such as isotherms, thermodynamics and kinetics studies validate the nature of adsorption process of TCP pollutant. The adsorption data found to be best fitted with Langmuir isotherms ($R^2 = 0.99$); whereas kinetic study suggested the pseudo-second-order nature of reaction with $R^2 = 0.99$. The thermodynamics study confirmed the spontaneous and endothermic nature of the TCP pollutant onto the surface of *p*-DMAC4/GO material. Moreover, the results of

---

* Corresponding author.
** Corresponding author.
*E-mail addresses:* awais.phy@hu.edu.pk (A. Khalid), ayazmemon33@usindh.edu.pk (A.A. Memon).

current work were also compared with existing reported adsorbents and data suggested the higher efficiency, feasibility, and reusability of *p*-DMAC4/GO material to remove the TCP pollutant from the wastewater system.

## 1. Introduction

Nowadays, one of the global issue in environmental system is the water pollution and contamination which released by several industrial sectors [1,2]. Since, numerous hazardous environmental contaminates are discharged into aqueous environment without any adequate treatment from different industrial sectors including petrochemical dyes, pharmaceuticals, dyes, agricultural that can pose adverse effects on human nervous system and cause so many health disorders in human as well as aquatic environment [3–5]. Among various pollutants, chlorophenols containing groups are highly toxic and teratogenic organic compounds due to their structural stabilization, difficult in degradation, bioaccumulation through food chain system and potential carcinogenic properties [6,7]. The wide use of chlorophenol compounds in different areas including plastics, dyes, pesticides, pharmaceuticals products, wood preservatives, fungicides, leather and steel industries that lead inevitable emission of chlorophenol compounds into the aquatic environment [8]. However, chemically known as 2,4,6-Trichlorophenol (TCP) as shown in Fig. 1 is very important pollutant among various chlorophenols which has various toxic, mutagenic and carcinogenic pollutant [9]. Moreover, the discharge of the 2,4,6-Trichlorophenol contaminated wastewater into aqueous system causes many diseases such as respiratory, cardiovascular, gastrointestinal effects bronchitis and chronic effects [10,11]. This is due to its highly stable C–Cl bond and the position of the chlorine atoms relative to the hydroxyl group is responsible for their toxicity and persistence in the biological environment. Also, the U.S environmental protection agency has classified as a major environmental pollutant because of its high toxicity, carcinogenic properties, and structural stabilization system [12]. Therefore, it is very important to develop a cost-effective method for the removal of 2,4,6-Trichlorophenol pollutant from aqueous system.

Currently, several analytical methods have been used for the effective removal of 2,4,6-Trichlorophenol from aqueous system such as ion exchange [13], degradation [14], oxidation [15], electrolysis [16], biological treatment and anaerobic granular sludge [17]. These analytical methods have certain disadvantages including high cost, ineffective and expensive, thus these methods are not suitable for industries operating at small level. Moreover, among these traditional developed methods the adsorption of TCP from wastewater is one of the most recommended methods because of its capability, simplicity, and reusability, cost-effective and quick oxidation than other methods [18,19].

A lot of research has been constructed on graphene oxide (GO) in past decade due to its outstanding properties such as high surface area, high electron mobility, good transmittance, unique optical, mechanical, electronic and other chemical and physical properties, compared to the other nanomaterials [20–22]. Due to these properties graphene oxide is used in different advanced fields of science and engineering such as biosensors, fuel cells, energy storage applications, catalysis, photonic, organic light emitting diodes, proactive coatings and contamination purification in wastewater management [23]. The graphene oxide contains various functional groups on its skelton including hydroxyl, carboxyl, and epoxy which further enhanced its chemical and physical properties [24]. Furthermore, different surface functionalization agents have been employed on the surface of graphene oxide such as metal carbide, organic polymers, biomolecules carbon nanotubes, and metal/metal oxide nanoparticles to enhance its stability and properties [25–28]. But among them, calixarene is the third generation supramolecular host compound after the crown ethers and cyclodextrins [29]. However, calixarenes and their derivatives have unique complexation abilities that allow for recognition of target molecules with high selectivity and efficient supramolecular recognition as well [30,31]. Moreover, they contain numerous cavity dimension with possibility to functionalization their upper and lower rim with different functional groups to improve its properties and to tailor their strong interaction with a target host molecules through different non-covalent interaction such as hydrogen bonding, π - π stacking, cation- π and CH-π interaction with the surface of target molecule [32–34]. Consequently, the incorporation of calixarene and its derivatives with the graphene oxide have become promising platform in various areas of research including sensing, electronics, separation, molecular recognition and adsorption of different organic and inorganic compounds from the aqueous environment [35,36]. Hence, the chemical immobilization or incorporation of calixarene derivatives on the surface of graphene oxide not only provides thermal
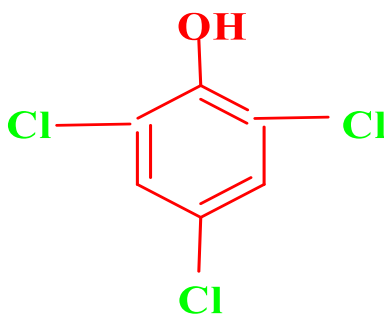


**Fig. 1.** Shows chemical Structure of 2,4,6 tri-chloro phenol.

stability but also enhanced adsorption properties for the removal of organic pollutant *i.e.* TCP from the aqueous system [37]. In addition, the large surface area of *p*-DMAC4/GO composite provides the more active sites for the 2,4,6-trichlorophenol pollutants to attach and enchaining the adsorption efficiency; *p*-DMAC4/GO composite is low-cost and sustainable material that can be synthesized using readily available raw materials. This makes them an attractive options for adsorption of 2,4,6-trichlorophenol environmental pollutant as they offer a cost-effective and eco-friendly solution and *p*-DMAC4/GO composite has been shown to exhibit good stability and reusability, making them effective in multiple cycles of adsorption and regeneration. This reduces the overall cost of using these materials for 2,4,6-trichlorophenol pollutant removal and makes them a practical solution for environmental remediation.

To best of our knowledge there is no example of dimethyl functionalized calix [4]arene based graphene oxide being used as adsorbent for the TCP. In this work, authors have synthesized *p*-DMAC4 functionalized graphene oxide based composite material first time using simple and cost-effective method for the removal of TCP from aqueous environment. The synthesized *p*-DMAC4 functionalized graphene oxide-based adsorbent removes 96% TCP from aqueous environment at pH 6.

## 2. Materials and method

### 2.1. Reagents

All the reagents were of analytical grade and used as supplied by without further purification. *p-tert*-butyl phenol, formaldehyde (37%), NaOH (98%), toluene, AlCl$_3$, HCl (35%), H$_2$SO$_4$ (96%) tetrahyderofuran (THF), glacial etic acid and dimethyl amine were purchased from the Sigma Aldrich, Germany). However, the graphite powder, NaNO$_3$, KMnO$_4$ and H$_2$O$_2$ (33%) were obtained from (Merck, Germany). Furthermore, the 2,4,6-tri-chloro phenol (TCP) was obtained from the (Arcos Organic, Belgium). Ultra-pure water was used for the preparation of all solutions.

#### 2.1.1. Synthesis of 5,11,17,23-dimethylamine-25,26,27,28-hydroxycalix [4]arene (p-DMAC4)

*p*-Tert-butyl calix [4]arene (**1**) and tetra-hydrxyocalix [4]arene (**2**) were synthesized by following previously reported literature [38]. While, the calix [4]arene derivative (**3**) was also synthesized via using previously reported method with some variations [39]. Briefly, 2 g (4.716 mM) of compound (**2**) were dissolved in 70 mL of THF followed by the addition of 10 mL glacial etic acid and 20 mL of Formaldehyde (37%) in the round bottom flask for 30 min at 0 °C. Then, the 3 mL of dimethylamine was added in the reaction mixture and left the reaction mixture at room temperature for 24 h. The reaction was monitored through the TLC by using solution mixture of (n-hexane &acetone 1:4). TLC study confirms the successful preparation of desired product. After that, the rotatory evaporator was used to remove the solvent from the reaction mixture and 100 mL de-ionized water added into the separate funnel to form two layers. Afterward, the two layers separated out by using twice (2 × 50 mL) with diethyl ether. Finally, the extracted solution neutralized with the 10% solution of K$_2$CO$_3$ and resulting precipitated product was filtrated off through whatmman filter paper. The recrystallization of product from chloroform: methanol system gave the pure compound **3** as shown in Scheme 1. Moreover, the conformation of structure and purity of **3** was done through different analytical techniques including melting point, TLC and FT-IR analysis.
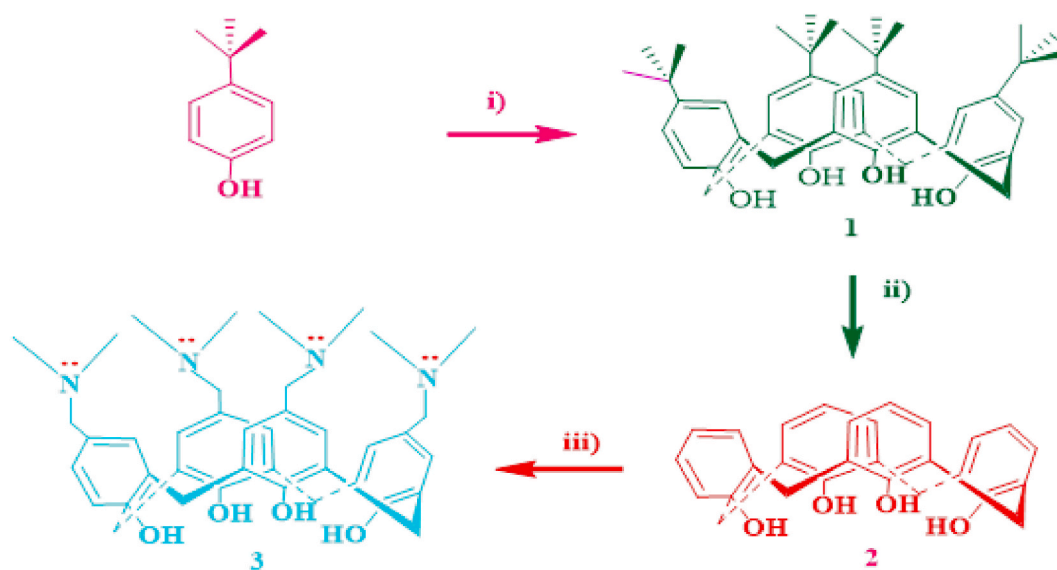


**Scheme 1.** Synthetic methodology for the synthesis of *p*-DAMC4 derivative by using following reaction conditions (i) HCHO/NaOH (ii) phenol-AlCl$_3$/(dry) Toluene and (iii) N, N-dimethylamine-HCHO/acetic acid: THF.

## 2.2. Preparation of graphene oxide (GO)

GO was prepared from natural graphite powder according to improved Hummer's method [40]. In typical synthesis procedure, 3 g of graphite powder was added in the 96 mL of conc: $H_2SO_4$ acid and added the 1.5 g of $NaNO_3$ at $^oC$ for 3 h in the ice bath with vigorously stirring with magnetic stirrer. After that, 9 g $KMnO_4$ was added slowly into reaction mixture to avoid the explosion and left the solution mixture for stirring for 1.5 h, and rise the temperature of solution mixture up to 35 $^\circ$C for 2 h. Afterward, 2 h gradually added the 138 mL de-ionized water and again added 420 mL of DI water with 3 mL of $H_2O_2$ (30%) into the reaction mixture with continues stirring to obtained the graphene oxide suspension. Next, the obtained suspension product of graphene oxide further washed with 3% HCl solution in order to removing the remaining metal contaminates from the product and leave for 10 days into dialysis tube to neutralize the obtained product. Later, the tip sonication (200 W) was employed to exfoliate the graphite into GO suspension. Finally, the GO suspension was centrifuge at 4000 rpm for 20 min to remove the remaining impurities from the suspension and to separate out the thick multilayered flakes respectively (see ).

## 2.3. Synthesis of p-DMAC4 graphene oxide composite (p-DMAC4/GO)

Scheme 2 shows the synthetic route of *p*-DMAC4/GO, firstly, *p*-DMAC4 was prepared according to reported method with minor modification [39]. Briefly, 0.2 g graphene oxide was added into a de-ionized water (50 mL DI) followed by ultra-sounding for 2 h in order to become homogeneity solution. Then, 70 mg of *p*-DMAC4 was added into above mixture solution under sonication for 1 h in such way that the *p*-DMAC4 reacts with GO solution and mixed well. Afterward, the resulting mixture was left for heat with continous stirring for 24 h. Then, the resulting mixture was kept in vacuum oven at 65 $^\circ$C for 3 h to become dried. Finally, the obtained product washed several times with mixture of methanol and de-ionized water to remove the remaining contaminates from product.

## 2.4. Characterization

Different analytical techniques have been used to confirm the successful synthesis of *p*-DMAC/GO composite. The chemical composition and surface interaction of prepared *p*-DMAC/GO composite was determined by using Fourier-transform infrared (FT-IR) spectroscopy (Thermo Nicolet 5700). However, the phase purity and crystalline nature of prepared composite was investigated via employing X-ray powder Diffraction (XRD-7000 Shimadzu-Scientific instrument) with Cu Kα radiation at scanning rate of 4° min$^{-1}$. Moreover, the surface morphology and elemental composition of prepared material was examined through the scanning electron microscopy with EDS detector (Nova Nano SEM, Japan, and Tokyo). The initial and final concentration of TCP was monitored by using UV–Visible spectrometer at wavelength 310 nm (PerkinElmer Lambda 35).
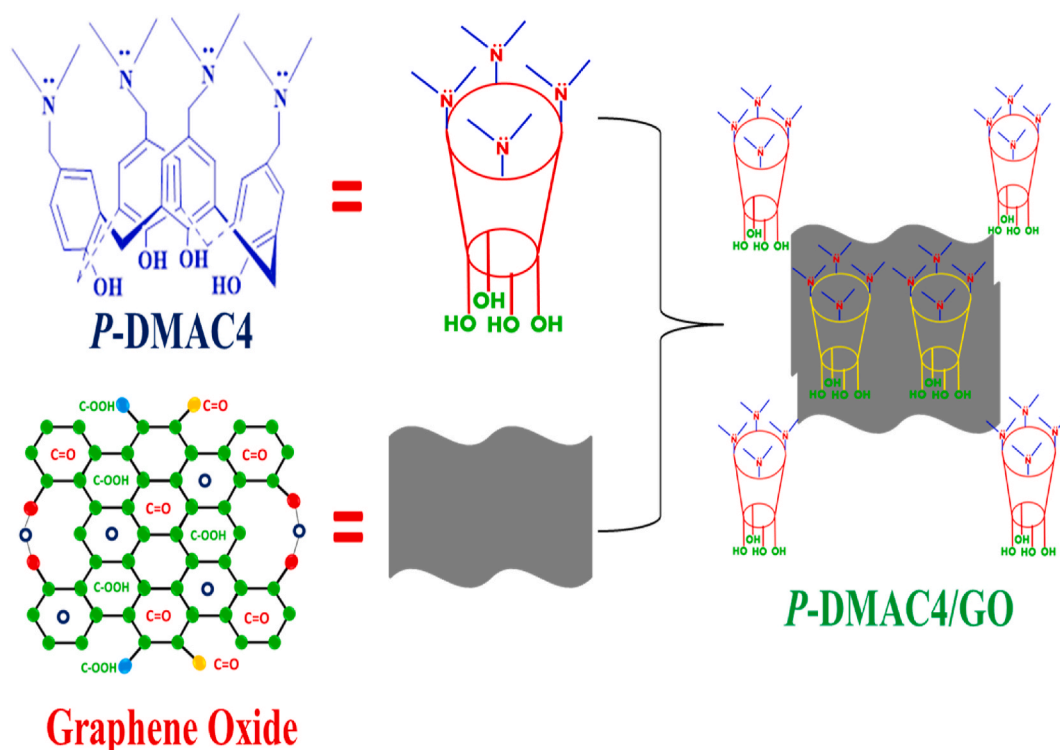


**Scheme 2.** Shows proposed interaction of *p*-DMAC4 with Graphene oxide surface.

### 2.5. Batch adsorption measurements

Batch adsorption was carried out for TCP at ambient temperature via using 10 mL solution of TCP with 50 ppm (50 mg $L^{-1}$) concentration and 10–50 mg of the adsorbent into 25 mL Erlenmeyer flask within pH range 2–10. The solution was shaken into incubator shaker for 60 min. After, the adsorption experiment the adsorbent was separated from the supernatant via employing centrifuge at 4000 rpm. Then, separated supernatant was analyzed for TCP residual concentration by taking its absorbance at $\lambda_{max}$ 310 nm via employing the UV–Visible spectrometer. Moreover, the removal % and adsorption capacity of TCP calculated by using equation **(1)** and **(2)** as given below.

$$\% \text{ adsorption} = \text{Xi} - \frac{\text{Xf}}{\text{Xi}} \times 100 \qquad (1)$$

Here, $X_i$ is the initial concentration of TCP solution and $X_f$ represent final concentration of TCP.

$$q_e = \frac{C_i - C_e}{m} \times V \qquad (2)$$

whereas $q_e$ = equilibrium adsorption capacity, $C_i$ is TCP concentration (mg/L) at time = 0, $C_e$ is the concentration of TCP (mg/L) at equilibrium, $V$ is the volume of the TCP solution (L), $m$ is the mass of adsorbent in (mg).

## 3. Results and discussion

### 3.1. FT-IR studies

The FT-IR spectroscopic technique is widely applicable for functional group analysis and changes in functionalities before and after reaction mechanism. Hence, functional groups on the surface of GO, *p*-DMAC4 and *p*-DMAC4/GO composite were examined with the help of FT-IR analysis. <b>Fig (2a),</b> shows the FT-IR spectra of GO. The broad peak at 3413 $cm^{-1}$ was corresponding to hydroxyl (OH) functional group. While the two peaks at 1640 and 1600 $cm^{-1}$ were assigned for the carbonyl (C=O) and aromatic carbon double bond (C=C), respectively. Furthermore, the peaks at 1428, 1220 and 1020 $cm^{-1}$ were attributed to the bending stretching of hydroxyl (OH) and carbon oxygen existing (C–O) functionalities of GO, respectively. Furthermore, the FT-IR spectra of *p*-DMAC4 containing numerous functional groups in its structure as shown in **Fig (2a)**. The broad band at 3400 $cm^{-1}$ was assigned for the hydroxyl (OH) stretching vibrations because of intra-molecular hydrogen bonding of the phenolic group. On other hand, two bands appearing at 2940 and 2850 $cm^{-1}$, respectively represent the asymmetrical and symmetrical stretching vibration of bridged methylene (CH$_2$) groups. While the peak at 1345 $cm^{-1}$ was assigned for C–N, and the band at 1588 and 1438 $cm^{-1}$ represent to C=C and C–H groups of aromatic ring, band at 1100 and 1040 $cm^{-1}$ shows the C–O. However, **Fig (2a)** clearly indicates the appearance of new peaks and vanishing of some peaks from the FT-IR spectra of *p*-DMAC4 after the interaction with the surface of GO. Though, it was noticed that the peak of C–N vanished and new peaks were appeared at 1380 and 1240 $cm^{-1}$ which show that *p*-DEAC4 was successful interacted with the surface of GO. Also, some vibrational absorption bands of GO appeared which confirmed the chemical interaction of GO with the surface of *p*-DMAC4.
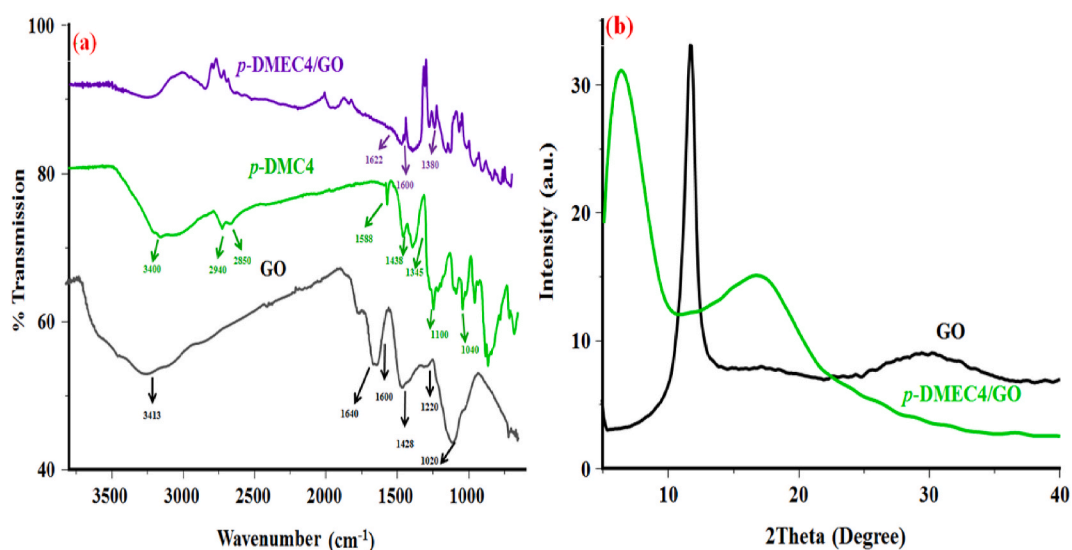


**Fig. 2. (a)** FT-IR spectrum of GO, *p*-DMAC4 derivative and *p*-DMAC4/GO after functionalization with GO **(b)** XRD patterns for GO and *p*-DMAC4/GO composite.

## 3.2. X-ray diffraction (XRD) analysis

X-ray Diffraction technique is used to evaluate the changes in crystallographic structure of a material. The crystal orientation and phase composition of synthesized *p*-DMAC4/GO composite material were analyzed by using XRD. The signal diffraction pattern of GO reveals a diffraction peak centered at $2\theta = 11.4°$ that corresponds to an interlayer distance (d-spacing) of 0.78 nm which indicating the presence of water molecules and oxygen containing functionalities in the GO Skelton as display in **Fig (2b)**. Moreover, the *p*-DMAC4/GO shows XRD diffraction pattern peak at $2\theta = 7.0$ with interlayer distance 1.2 nm as display in Fig **(2b)**. Additionally, the crystallite size of prepared GO and *p*-DMAC4/GO composite material were determined by using Debye Scherrer formula, the equation (3) is given below. Where D is the crystalline size of nanocomposite, K represents the Scherrer constant (0.98), $\lambda$ denotes the wavelength (1.54), $\beta$ denotes the full width at half maximum (FWHM). The average grain size of prepared GO and *p*-DMAC4/GO composite were calculated theoretically by using above given formula to be of GO 25 nm and *p*-DMAC4/GO composite material 30 nm.

$$D = \frac{K\,\lambda}{\beta\,Cos\,\theta} \tag{3}$$

## 3.3. Scanning electron microscopy (SEM)

Scanning electron microscopic technique is widely used to study the surface phenomenon and to monitor surface morphological changes in any material on completion of any reaction. Hence, to obtain the detailed information about the roughness and surface morphology of synthesized GO and *p*-DMAC4/GO composite material, scanning electron microscopy (SEM) measurement was carried out as shown in <b>Fig (3a,b,c,d)</b>. Fig **(3a, b)** represents the SEM images of GO before incorporation of *p*-DEAC4 having uniform and smooth topography. Moreover, the SEM images of *p*-DEAC4/GO formation of typical hybrid composite material, in which the *p*-DEAC is uniformly distributed over the surface of GO and its roughness attributes its applicability as potential adsorbent for TCP, as shown in **Fig (3c, d)**. Furthermore, the Energy-Dispersive X-ray spectroscopy (EDS) was used to determine the elemental composition of the synthesized material. The EDS pattern of *p*-DMAC4/GO **Fig (3e)** shows the presence and uniform distribution of C, O and N elements on the surface of GO. Therefore, these results confirmed the successful synthesis and encapsulation of *p*-DMAC4/GO without any other impurity in the product.

## 3.4. Adsorption study

### 3.4.1. Effect of pH

The influence of pH plays a key role in all chemical processes. Therefore, to determine the effect of pH on adsorption of 2, 4, 6-trichloro phenol (TCP), the point of zero charge for synthesized *p*-DMAC4/GO composite material was investigated. Hence, for that NaNO$_3$ buffer of 0.5 M concentration was prepared with pH values ranging from 3 to 10 in different flasks, to each flask the appropriate amount of composite material (30 mg) was added and shacked for 20 h at ambient temperature at 60 rpm. Afterward, the adsorbent material was separated out through whatmman filter paper and final pH of buffer solution was checked. After that, the point of zero charge of adsorbent material was calculated as 8.0 which highlights negative charge on the surface of adsorbent material as shown in Fig. (4a). Moreover, the pH of aqueous solution is a vital parameter which is used to determine the adsorption capacity of adsorbent for
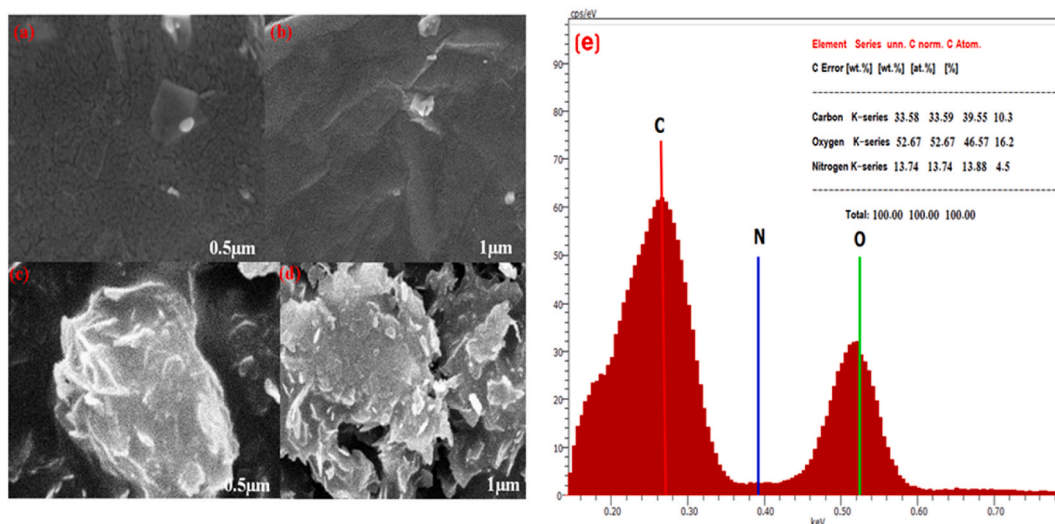


**Fig. 3.** (a, b) SEM image of GO **(c, d)** SEM image of *p*-DMAC4/GO at high and low resolution.**(e)** EDS elemental pattern of *p*-DMAC4/GO composite material.

the wastewater treatment [41]. The effect of pH on the removal of 2, 4, 6-trichloro phenol (TCP) was carried out with pH ranging from 2 to 10 as shown in Fig. (b). The results revealed that the adsorption process of TCP is pH dependent. However, the %adsorption of TCP increases as the pH increases from 2 to 6 and attains its maximum at pH 6 followed by sharp decline in %adsorption from pH of 7–10. This phenomenon can be explained from the fact of existing charge on the surface of adsorbent and the various stat of TCP at different pH values. Moreover, the p*k*a value of TCP (6.23) reveals that the maximum adsorption occurred at pH 6 because of the higher content of TCP. While the increase in the pH value of TCP solution effectively increases the fraction of negative charge on TCP that tends the decline in %adsorption of TCP from wastewater. Moreover, the adsorbent containing different oxygen functionalities on its surface and some the anionic groups may be deprotonated at higher pH value resulting the negative charge on surface of the adsorbent material also responsible for the decline in adsorption of TCP at higher pH value. Therefore, the electrostatic repulsion of anionic TCP with negative charged surface of adsorbent material makes the adsorption process unfavorable. So, all remaining parameters were carried out at optimum pH value of 6 for TCP for wastewater treatment.

### 3.4.2. Effect of adsorbent dosage

Another major parameter used for establishing the efficiency of an adsorbent is its adsorption capability for TCP from wastewater. Therefore, to check the effect of adsorbent dosage, the amount of adsorbent material varied from 10 to 50 mg while all other parameters such as pH, contact time, initial concentration and temperature remained constant. As shown in **Fig (5a)** the % adsorption of TCP is increasing markedly by the increase in amount of the adsorbent martial and maximum adsorption is obtained at 30 mg that remains constant till 50 mg, this is because of the fact that for available concentration of TCP, 30 mg is sufficient for its adsorption, hence increased amount of adsorbent does not show any additional change in %adsorption. Therefore, the 30 mg adsorbent amount was taken as optimum amount of adsorbent material for further studies.

### 3.4.3. Effect of shaking time

Contact time or equilibrium time has great influence on the %adsorption. To study the effect of contact time on removal of TCP from wastewater using p-DMAC4/GO as adsorbent material, the contents were agitated from 30 to 150 min. Fig. (5b) shows the % adsorption is increasing by increasing the shaking time and equilibrium is established within 60 min, that decreases with further increase in contact time that might be because of the desorption takes place due to agitation for excessive time. Therefore, 60 min shaking time is considered as optimum for the maximum %adsorption of TCP pollutant.

### 3.4.4. Adsorption isotherms

The adsorption isotherms are used as empirical models to describe the adsorption equilibrium of adsorbate on the surface of adsorbent. Presently, adsorption isotherm models have been used to evaluate the affinity of adsorbent material towards adsorbate and how the adsorbate ions are dispersed between the liquid solution and the adsorbent material in the equilibrium phase. Therefore, in this study Langmuir and Freundlich isotherms models were used to evaluate the adsorption isotherms of the designed system.
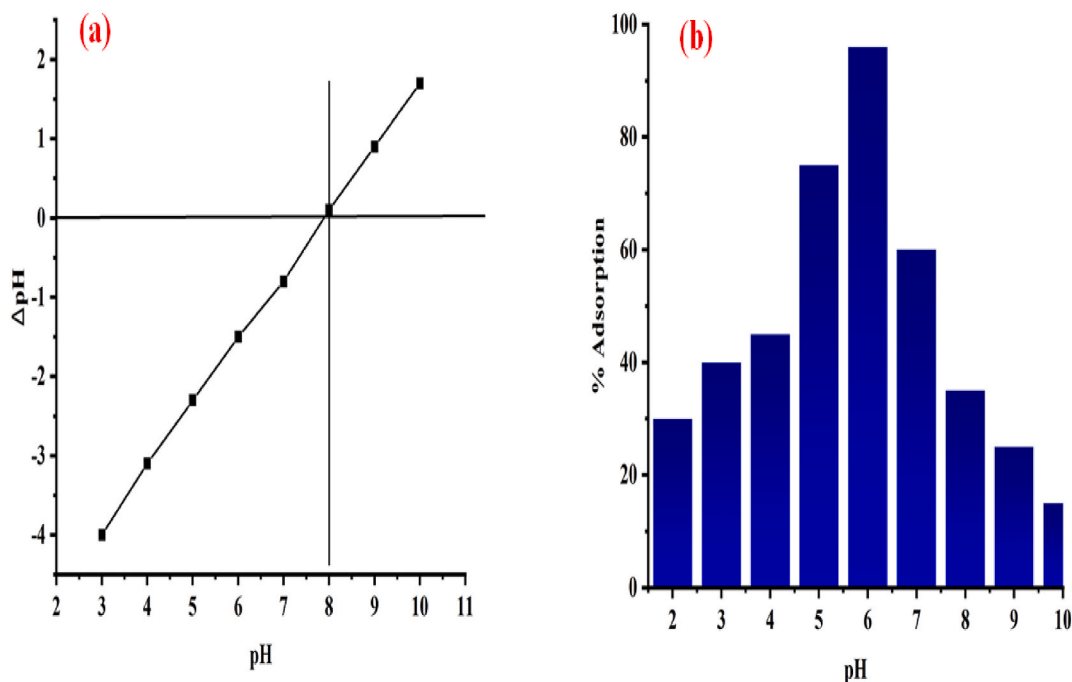


**Fig. 4. (a)** Point of zero charge on p-DMAC4/GO composite material **(b)** Influence of pH on the adsorption of TCP pollutant.
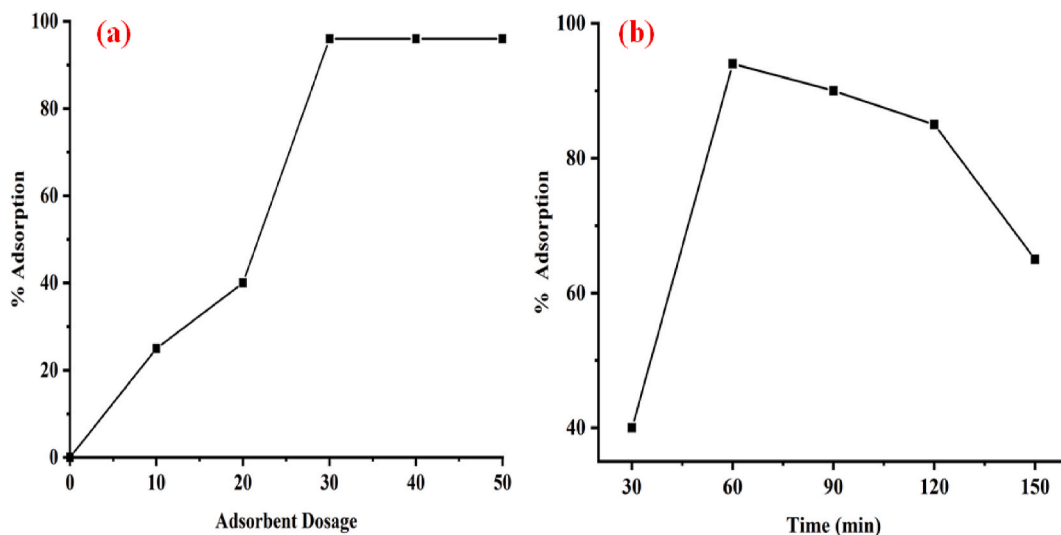
**Fig. 5. (a)** Effect of adsorbent dosage **(b)** Effect of shaking time on the adsorption of TCP pollutant onto *p*-DMAC4/GO composite material.

### 3.4.5. Langmuir isotherms model

The Langmuir isotherm study is used to explain the adsorption process that occurs on homogenous surface of the adsorbent material and assumes that adsorption process is monolayer adsorption in nature [42]. The Langmuir isotherm model equation is expressed as below **(4)** [43].

$$\frac{C_e}{C_{ads}} = \frac{1}{Qb} + \frac{C_e}{Q} \tag{4}$$

where $C_e$ equilibrium concentration (mol·L$^{-1}$), $C_{ads}$ is sorbed concentration (mg·g$^{-1}$), $Q$ is monolayer sorption capacity (mol·g$^{-1}$), $b$ is the Langmuir constant. A plot of $C_e/C_{ads}$ versus $C_e$ exhibits straight line with slope *1/Q* and intercept *1/Qb* as shown in Fig. (6a).

Also the important aspect of the Langmuir isotherm model is often indicated as a dimensionless factor, $R_L$ which can be expressed as below equation **(5)** [44].

$$R_L = \frac{1}{1 + bCi} \tag{5}$$

whereas, $R_L$ shows the nature of adsorption process favorable or unfavorable. However, for favorable adsorption process the value of $R_L < 1$, unfavorable the value of $R_L > 1$, linear for $R_L = 1$ and irreversible $R_L$ value is $= 0$.
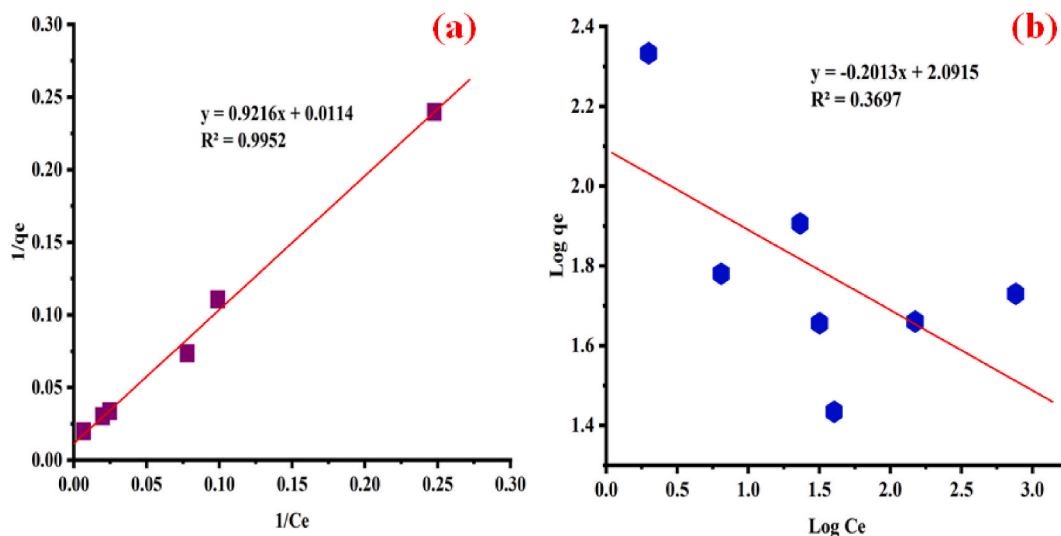


**Fig. 6. (a)** Langmuir Isotherms **(b)** Freundlich Isotherms for TCP adsorption onto *p*-DMAC4/GO composite material.

8

### 3.4.6. Freundlich isotherm model

Freundlich isotherm model was used for adsorption process to determine the heterogeneous surface containing binding sites to their various energies and multilayer adsorption sites of the adsorbent material. The Freundlich isotherm model expression is as follows (6) [45].

$$\log C_{ads} = C_m + \frac{1}{n} \log C_e \tag{6}$$

where $C_{ads}$ is adsorbed concentration (mol·g$^{-1}$), $C_m$ is multilayer sorption capacity $1/n$ is sorption intensity, and $C_e$ is an equilibrium concentration (mol·L$^{-1}$). A plot of log $C_{ads}$ versus $C_e$ exhibits straight line with slope $1/n$ and intercept $C_m$ as shown in <b>Fig (6b).</b>

If value of n > 1 which indicates the adsorption process favorable according to Freundlich isotherm model.

Favorability and unavoidability of adsorption process can be evaluated from isotherm constants [46]. The value of adsorption intensity ($1 < n < 10$) indicates favorability of adsorption. The corresponding value of $n$ for TCP adsorption is 5.18, which reveals the adsorption is favorable. Moreover, favorablity of adsorption can also be evaluated from the calculated value of R$_L$ (0.286), that is < 1. In addition, the value of $R^2$ is higher in Langmuir as compared to Freundlich model, which indicate that adsorption of TCP favors the Langmuir isotherm. Moreover, the applicability of both isotherms can also be evaluated on the basis of their calculated adsorption capacities, that the value is higher for Langmuir isotherm as compared to Freundlich isotherm. Consequently, the Langmuir isotherm model is suggested as favorable which defines monolayer coverage of the TCP pollutant on the surface of *p*-DMAC4/GO composite material. The values of constants obtained from both the sorption models are given in Table 1.

### 3.4.7. Thermodynamics of adsorption

The thermodynamics of the adsorption is important for understanding the nature of the adsorption process because temperature has significant influence on the adsorption of TCP from wastewater. The different thermodynamics parameters such as enthalpy ($\Delta H^0$), entropy ($\Delta S^0$) and Gibbs free energy ($\Delta G^0$) were calculated by using equation (7), and their values are presented in Table 2. The thermodynamics study is carried out in the range of 296–334 K.

$$\ln Kc = -\frac{\Delta H}{RT} + \frac{\Delta S}{R} \tag{7}$$

The negative value of $\Delta \overset{o}{G}$ for the adsorption process at all temperature suggested that adsorption process of TCP pollutant onto *p*-DMAC4/GO adsorbent material is spontaneous process and is thermodynamically favorable. As shown in Table 2, the enthalpy change ($\Delta H^0$) for the TCP adsorption was found to be 18.43 KJmol$^{-1}$ that indicates the adsorption process is endothermic in nature. Moreover, the value of $\Delta S$ = 64.23 JK-1mol$^{-1}$ reveals the increased randomness at the solid-liquid interface during the adsorption process of TCP pollutant onto the surface of *p*-DMAC4/GO composite material [54,55].

### 3.5. Kinetics of adsorption

To understand the better adsorption efficiency of the *p*-DMAC4/GO composite material towards the TCP pollutant; the effect of contact time on the adsorption process was studied. Also, the adsorption kinetics study is used to predict the rate-controlling step in overall adsorption process and contact time gives meaningful information for modeling and designing the adsorption process. Pseudo-first-order and Pseudo-second-order models were used for the kinetic studies of TCP pollutant onto the surface of *p*-DMAC4/GO composite material. Moreover, the Lagergren (pseudo-first-order) equation (8) [56] and HO and Mckay (Pseudo-second-order) equation (9) [57] were used for the calculation of mathematical values for adsorption kinetics studies as given below.

$$\log(q_e - q_t) = \log q_e - \frac{k_1 t}{2.303} \text{ Lagergren model} \tag{8}$$

$$\frac{t}{q_t} = \frac{1}{k_2 q_e^2} + \frac{t}{q_e} \text{ H}_o \text{ and McKay model} \tag{9}$$

where $q_e$ and $q_t$ are amount of TCP adsorbed at equilibrium time (mgg$^{-1}$) and given time t respectively; $k_1$ (min$^{-1}$) and $k_2$ (gmg$^{-1}$ min$^{-1}$) are the rate constants of the pseudo-first-order and pseudo-second-order respectively.

The regression coefficient plots of two models for the adsorption of *p*-DMAC4/GO composite material towards the TCP pollutant is shown in <b>Fig (7a, b)</b>. Moreover, the regression coefficient of pseudo-seconder-order equation $R^2$ **(0.99)** is much better than that of the pseudo-first-order equation $R^2$ **(0.33)** which indicating the pseudo-second-order model equation is much fitted than the

**Table 1**

Shows Values of the Langmuir and Freundlich isotherms models constants for the adsorption of TCP onto *p*-DMAC4/GO composite material.

| Langmuir Isotherm | | | Freundlich Isotherm | | |
| --- | --- | --- | --- | --- | --- |
| Q (mg/g) | b | $R^2$ | $C_m$ (mg/g) | 1/n | $R^2$ |
| 38.39 | 0.053 | 0.99 | 13.36 | 0.193 | 0.36 |

**Table 2**
Shows the Thermodynamics Parameters onto surface of *p*-DMAC4/GO composite material.

| Temperature (K) | $\Delta G^{\circ}$ (KJmol$^{-1}$) | $\Delta H^{\circ}$ (KJmol$^{-1}$) | $\Delta S^{\circ}$ (JK$^{-1}$mol$^{-1}$) |
|---|---|---|---|
| 296 | −1.99 | 18.43 | 64.23 |
| 316 | −3.17 | | |
| 336 | −4.60 | | |

pseudo-first-order model equation for the kinetic adsorption process of TCP on the surface of *p*-DMAC4/GO.

### 3.5.1. Real sample analysis

To check the applicability of *p*-DMAC4/GO composite material as an efficient adsorbent for the removal of TCP pollutant from real wastewater system, the wastewater samples are collected from the Jamshoro Industrial area containing the TCP as pollutant. The batch study was performed to determine the analytical applicability of *p*-DMAC4/GO composite material via optimum parameters (30 mg amount and 30 mL of wastewater samples stirred at 120 rpm for 60 min) in the Erlenmeyer flask. The concentration of the TCP pollutant before and after the treatment of TCP wastewater with the *p*-DMAC4/GO composite material was calculates through UV–Visible spectrometer at its $\lambda_{max}$ 310 nm and results are given in Table 3. It was revealed from given results that the *p*-DMAC4/GO composite material reduced the concentration of TCP pollutant from the wastewater system.

### 3.5.2. Comparative study with other adsorbent materials

A wide range of adsorbent materials have been employed for the removal of TCP pollutant from the aqueous system. Table 4 shows the results of present study compared with previously reported adsorbent materials. These results were compared in terms of adsorbent amount, pH, shaking time and maximum adsorption capacity. The newly synthesized *p*-DMAC4/GO composite showed excellent adsorption capacity and percent adsorption as reported adsorbent materials. Furthermore, the excellent reusability and adsorption capacity makes its outstanding adsorbent material for the removal of TCP pollutant from the wastewater system.

### 3.5.3. SEM and EDX analysis after adsorption of 2,4,6-trichlorophenol

The SEM and EDX analysis was carried out to determine the physical morphology of prepared *p*-DMAC4/GO composite material and the existence of 2,4,6-Trichlorophenol after adsorption. Fig. (8a) revealed the SEM image of *p*-DMAC4/GO composite material after the adsorption of 2,4,6-Trichloropheno, the morphology of adsorbent material remained same for the 2,4,6-Trichlorophenol. Fig. (8b) displayed the EDX spectra f 2,4,6-Trichlorophenol and confirmed the presence of adsorbed material on the surface of *p*-DMAC4/GO composite material.

### 3.5.4. Adsorption mechanism

The prepared *p*-DMAC4/GO composite material showed significant adsorption capacity for TCP pollutant from aqueous environment. The adsorption mechanism is highly pH dependent and seems to be chemical adsorption involved for the adsorption TCP pollutant from aqueous environment. Due to the interaction of hydroxyl group and π-π interaction TCP pollutant with the surface of *p*-DMAC4/GO composite material because *p*-DMAC4/GO composite containing –OH, O, N and π-π system as shown in Scheme 3.
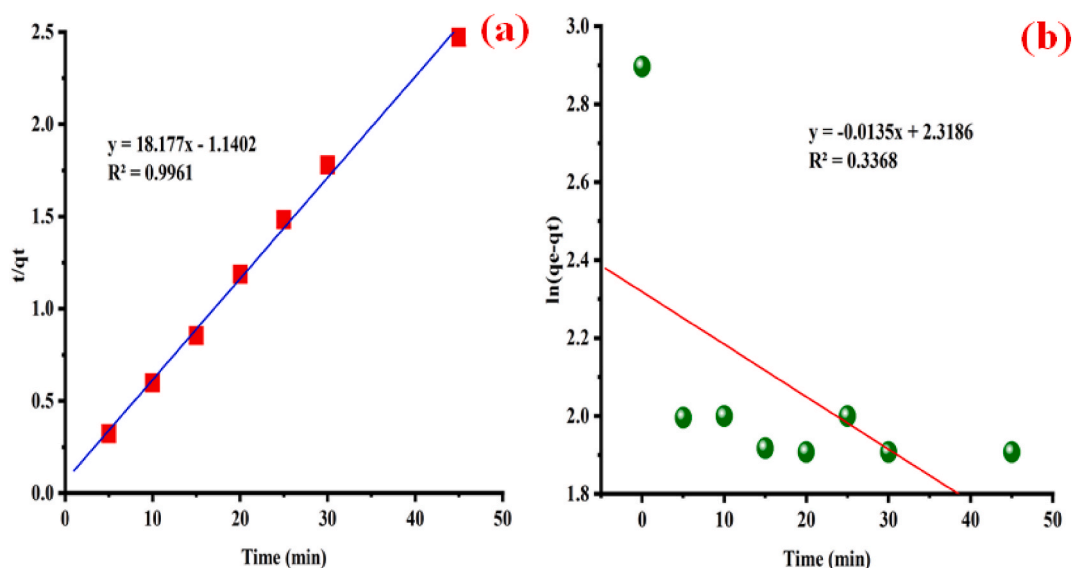


**Fig. 7. (a)** Pseudo-Second-order **(b)** Pseudo-First-order Plots of TCP Pollutant adsorption onto *p*-DMAC4/GO composite material.

**Table 3**

Shows the amount found and % removal of TCP pollutant from wastewater system via employing *p*-DMAC4/GO composite.

| Samples | Amount Found | % Removal |
|---|---|---|
| | 2,4,6-Tri-Chlorophenol (TCP) mg.L$^{-1}$ | 2,4,6-Tri-Chlorophenol (TCP) |
| **A** | 0.789 | 95.8 |
| **B** | 0.819 | 93.6 |

**Table 4**

Comparison of adsorption performance of *p*-DMAC4/GO with other adsorbent materials.

| Name of sorbent | Dosage of sorbent (mg) | Equilibrium Time (h) | pH | $q_{max}$ (mg/g) | Ref. |
|---|---|---|---|---|---|
| Albizia lebbeck (Rattle Seed) Pod | – | 2 | 3 | 6.80 | [47] |
| Activated Carbon prepared from Flamboyant pod bark | 200 | 1.5 | – | 37.64 | [48] |
| Chitosan | 300 | 4 | 6.5 | 20.41 | [49] |
| Azollafiliculoides biomass | 10,000 | 2 | 5 | 6.2 | [50] |
| Bentonite modified with benzyl dimethyl tetra decyl ammonium chloride | 50 | 1 | 4 | 35 | [51] |
| *Sargassum Boveanum* Macroalgae (MA) | 1000 | 6 | 5 | 10 | [52] |
| Surfactant-modified clinoptilolite– polypropylene hollow fiber composites | – | 24 | – | 64.5 | [53] |
| ***p*-DMAC4/GO** | **30** | **1** | **6.0** | **38.4** | **Present Work** |
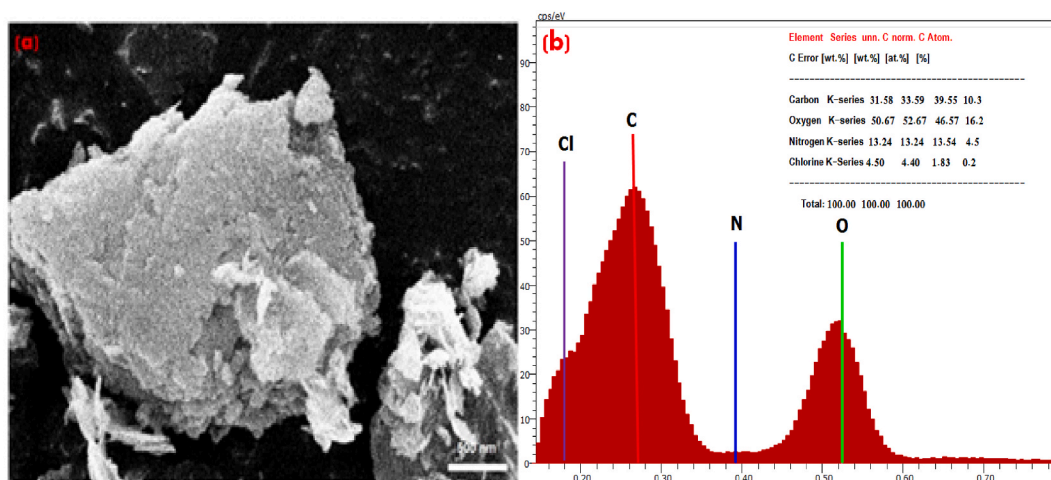


**Fig. 8. (a)** SEM image **(b)** EDX Spectra of *p*-DMAC4/GO composite material after the adsorption of 2,4,6-Trichlororphenol.

### 3.5.5. Reusability study

The reusability of the adsorbent material is most important that influence the energy cost and removal of pollutant from the aqueous system. Moreover, the reusability of the *p*-DMAC4/GO composite with continuous adsorption and recovery of TCP pollutant from wastewater system. After each adsorption process, the TCP pollutant was recovered from adsorbent material by using 5 mL of 0.1 M HCl solution shaking for 30 min. The removal capacity of the TCP pollutant was determined and obtained results revealed that the adsorption capacity significantly decreased after the five no. of cycles from 94 to 85% as shown in Fig. (9). Therefore, the excellent reusability of the synthesized *p*-DMAC4/GO material can use for the industrial application of various pollutant from aqueous system.

## 4. Conclusion

It could be conclude that novel *p*-DMAC4/GO composite material synthesized via using cost-effective strategy and characterized through various analytical tools. The synthesized *p*-DMAC4/GO composite material employed as an effective adsorbent for the removal of 2, 4, 6-trichlorophenol pollutant (95%) from the wastewater at optimum parameters. The adsorption of TCP is highly pH dependent and maximum adsorption achieved at pH 6.0. Furthermore, the isotherm models, kinetic and thermodynamics studies further confirm experimental results. Consequently, these findings indicate that the *p*-DMAC4/GO composite material is a highly suitable adsorbent for various large-scale environmental applications to remove different types of pollutants from aqueous systems, in
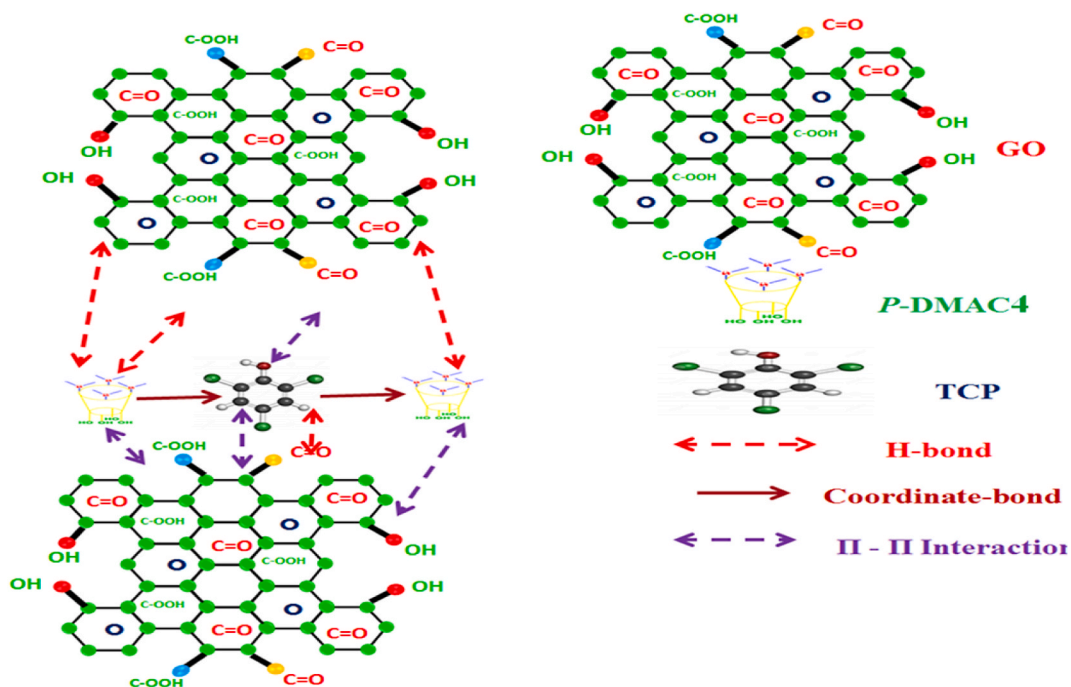
**Scheme 3.** Proposed interaction of *p*-DMAC4/GO composite with 2,4,6-tri chloro phenol (TCP).
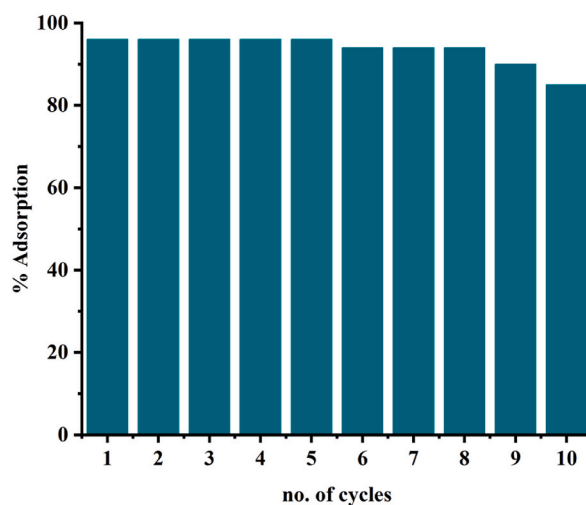


**Fig. 9.** Reusability study of the *p*-DMAC4/GO composite material with various no.of cycles.

comparison to a number of previously reported methods. Overall, this study presents a promising approach for effective and efficient wastewater treatment, with potential for practical applications in the future.

**Author contribution statement**

Ali Hyder, Dahar Janwery: Performed the experiments; Wrote the paper.

Muzamil Thebo, Jamil Ahmed Buledi, Imamdin Chandio: Contributed reagents, materials, analysis tools or data; Analyzed and interpreted the data.

Awais Khalidd, Bader S. Al-Anzi, Hanadi A. Almukhlifi: Contributed reagents, materials, analysis tools or data; Wrote the paper.

Khalid Hussain Thebo, Fakhar N. Memon, Ayaz Ali Memon: Conceived and designed the experiments; Analyzed and interpreted the data; Wrote the paper.

Amber Rehana Solangi, Shahabuddin Memon: Analyzed and interpreted the data; Wrote the paper.

**Data availability statement**

Data included in article/supp. material/referenced in article.

**Declaration of competing interest**

The authors declare that they have no known competing financial interests or personal relationships that could have appeared to influence the work reported in this paper.

**Acknowledgement**

**References**

[1] C.P. Okoli, P.N. Diagboya, I.O. Anigbogu, B.I. Olu-Owolabi, K.O. Adebowale, Competitive biosorption of Pb (II) and Cd (II) ions from aqueous solutions using chemically modified moss biomass (Barbula lambarensis), Environ. Earth Sci. 76 (33) (2017) 1–10.

[2] C.P. Okoli, G.O. Adewuyi, Q. Zhang, P.N. Diagboya, Q. Guo, Mechanism of dialkyl phthalates removal from aqueous solution using γ-cyclodextrin and starch based polyurethane polymer adsorbents, Carbohydr. Polym. 114 (2014) 440–449.

[3] S. Madhav, A. Ahamad, A.K. Singh, J. Kushawaha, J.S. Chauhan, S. Sharma, P. Singh, Water pollutants: sources and impact on the environment and human health, Sens. Water Pollutants Monit.: Role Mater. (2020) 43–62.

[4] N.T. Tavengwa, B. Moyo, H. Musarurwa, T. Dalu, Challenges and Future Directions in the Analysis of Emerging Pollutants in Aqueous Environments, Emerging Freshwater Pollutants, Elsevier, 2022, pp. 373–379.

[5] A. Saravanan, P.S. Kumar, S. Jeevanantham, M. Anubha, S. Jayashree, Degradation of toxic agrochemicals and pharmaceutical pollutants: effective and alternative approaches toward photocatalysis, Environ. Pollut. (2022), 118844.

[6] A.D. Chandio, A.H. Pato, I.A. Channa, S.J. Gilani, A.A. Shah, J. Ashfaq, J.A. Buledi, I.A. Chandio, M.N.B. Jumah, Exploring the heterocatalytic proficiencies of ZnO nanostructures in the simultaneous photo-degradation of chlorophenols, Sustainability 14 (21) (2022). Article 14562.

[7] Y. Gucbilmez, Physiochemical Properties and Removal Methods of Phenolic Compounds from Waste Waters, Persistent Organic Pollutants (POPs)-Monitoring, Impact and Treatment, IntechOpen, 2022.

[8] Q. Zhao, H. Lv, Z. Cui, M. Zhao, B. Cui, D. Zhou, Riboflavin enhances the synergy of electroactive bacteria and fenton reaction, improving chlorophenol degradation and Fe circulation, ACS EST Water 2 (8) (2022) 1461–1470.

[9] A. Noor, A. Khan, H.N. Bhatti, M. Zahid, F. Aslam, A. Naouar, F.F. Al-Fawzan, S.A. Alissa, M. Iqbal, Polypyrrole and rice husk composite potential for the adsorptive removal of 2, 4, 6-trichloro phenol from aqueous medium, Arab. J. Chem. 15 (12) (2022), 104352.

[10] A. Jabeen, U. Kamran, S. Noreen, S.-J. Park, H.N. Bhatti, Mango seed-derived hybrid composites and sodium alginate beads for the efficient uptake of 2, 4, 6-trichlorophenol from simulated wastewater, Catalysts 12 (9) (2022) 972.

[11] N. Ghochlavi, A.A. Aghapour, Biodegradation of 2-4-6 trichlorophenol by sequencing batch reactors (SBR) equipped with a rotating biological bed and operated in an anaerobic-aerobic condition, Front. Environ. Sci. 10 (2022) 2053.

[12] L. Keith, W. Telliard, ES&T special report: priority pollutants: ia perspective view, Environ. Sci. & Techol. 13 (4) (1979) 416–423.

[13] M. Caetano, C. Valderrama, A. Farran, J.L. Cortina, Phenol removal from aqueous solution by adsorption and ion exchange mechanisms onto polymeric resins, J. Colloid Interface Sci. 338 (2) (2009) 402–409.

[14] S. Anandan, A. Vinu, T. Mori, N. Gokulakrishnan, P. Srinivasu, V. Murugesan, K. Ariga, Photocatalytic degradation of 2, 4, 6-trichlorophenol using lanthanum doped ZnO in aqueous suspension, Catal. Commun. 8 (9) (2007) 1377–1382.

[15] J. Jiang, Y. Gao, S.-Y. Pang, X.-T. Lu, Y. Zhou, J. Ma, Q. Wang, Understanding the role of manganese dioxide in the oxidation of phenolic compounds by aqueous permanganate, Environ. Sci. & Techol. 49 (1) (2015) 520–528.

[16] T. Murakami, Y. Hamasaki, Basic study of autologous-bone-replaceable artificial bone fabrication with porosity distribution using electrolysis, Int. Design Eng. Tech. Conf. Comput. Info. Eng. Conf. (2010) 433–438.

[17] S. Eker, F. Kargi, Biological treatment of 2, 4, 6-trichlorophenol (TCP) containing wastewater in a hybrid bioreactor system with effluent recycle, J. Environ. Manag. 90 (2) (2009) 692–698.

[18] W. Chen, L. Duan, L. Wang, D. Zhu, Adsorption of hydroxyl-and amino-substituted aromatics to carbon nanotubes, Environ. Sci. & Techol. 42 (18) (2008) 6862–6868.

[19] W. Chen, L. Duan, L. Wang, D. Zhu, Response to comment on "Adsorption of hydroxyl-and amino-substituted aromatics to carbon nanotubes", Environ. Sci. & Techol. 43 (18) (2009) 3400–3401.

[20] K. Thakur, B. Kandasubramanian, Graphene and graphene oxide-based composites for removal of organic pollutants: a review, J. Chem. Eng. Data 64 (3) (2019) 833–867.

[21] H. Deng, J. Huang, C. Qin, T. Xu, H. Ni, P. Ye, Preparation of high-performance nanocomposite membranes with hydroxylated graphene and graphene oxide, J. Water Process Eng. 40 (2021), 101945.

[22] F.A. Janjhi, D. Janwery, I. Chandio, S. Ullah, F. Rehman, A.A. Memon, J. Hakami, F. Khan, G. Boczkaj, K.H. Thebo, Recent advances in graphene oxide-based membranes for heavy metal ions separation, Chem. Bio. Eng. Rev. 9 (6) (2022) 574–590.

[23] A.G. Olabi, M.A. Abdelkareem, T. Wilberforce, E.T. Sayed, Application of graphene in energy storage device–A review, Renew. Sustain. Energy Rev. 135 (2021), 110026.

[24] M. Dahanayaka, J.W. Chew, Organic solvent permeation through negatively charged graphene oxide membranes, ACS Sustain. Chem. Eng. 10 (4) (2022) 1499–1508.

[25] H. Yu, H. He, G. Xiao, Y. Fan, J. Ma, Y. Gao, R. Hou, X. Yin, Y. Wang, X. Mei, The roles of oxygen-containing functional groups in modulating water purification performance of graphene oxide-based membrane, Chem. Eng. J. 389 (2020), 124375.

[26] P. Khanra, T. Kuila, N.H. Kim, S.H. Bae, D.-s. Yu, J.H. Lee, Simultaneous bio-functionalization and reduction of graphene oxide by baker's yeast, Chem. Eng. J. 183 (2012) 526–533.

[27] Z. Yu, L.T. Drzal, Functionalized graphene oxide as coupling agent for graphene nanoplatelet/epoxy composites, Polym. Compos. 41 (2020) 920–929.

[28] J.A. Buledi, A.R. Solangi, A. Hyder, N.H. Khand, S.A. Memon, A. Mallah, N. Mahar, E.N. Dragoi, P. Show, M. Behzadpour, Selective oxidation of amaranth dye in soft drinks through tin oxide decorated reduced graphene oxide nanocomposite based electrochemical sensor, Food Chem. Toxicol. 165 (2022), 113177.

[29] J.H. Lee, J. Park, J.-W. Park, H.-J. Ahn, J. Jaworski, J.H. Jung, Supramolecular gels with high strength by tuning of calix [4] arene-derived networks, Nat. Commun. 6 (2015) 1–9.

[30] N. Verma, P. Sutariya, T. Patel, M. Shukla, A. Pandya, Tailored calix [4] arene-gold nanoconjugate as a ultra-sensitive immunosensing nanolabel, Biomed. Microdevices 25 (1) (2023) 1–11.

[31] H. Soni, J. Prasad, A. Pandya, S.S. Soni, P.G. Sutariya, Disposable paper-based PET fluorescence probe linked with calix [4] arene for lithium and phosphate ion detection, New J. Chem. 46 (2022) 21115–21123.

[32] J.-L. Liu, M. Sun, Y.-H. Shi, X.-M. Zhou, P.-Z. Zhang, A.-Q. Jia, Q.-F. Zhang, Functional modification, self-assembly and application of calix [4] resorcinarenes, J. Inclusion Phenom. Macrocycl. Chem. 102 (2022) 1–33.

[33] Y. Ali, N.M. Eltayeb, S.M. Salhimi, M. Taher, S. Abd Hamid, Synthesis, Molecular docking and antiproliferative activity of upper rim modified azo calix [4] arene derivatives, J. Inclusion Phenom. Macrocycl. Chem. 102 (2022) 873–880.

[34] V.S. Saji, Recent updates on supramolecular-based drug delivery–macrocycles and supramolecular gels, Chem. Rec. 22 (7) (2022). Atricle 202200053.

[35] H. Abbassi, M. Mezni, R. Abidi, M. Benna-Zayani, Synthesis and characterization of calix [4] arene diester-grafted-functionalized clay nanocomposites, Phys. Chem. Lett. 809 (2022), 140153.

[36] M.A. Kamboh, W.A. Wan Ibrahim, H. Rashidi Nodeh, L.A. Zardari, M.M. Sanagi, Fabrication of calixarene-grafted magnetic nanocomposite for the effective removal of lead (II) from aqueous solution, Environ. Technol. 40 (2019) 2482–2493.

[37] C. Liu, D. Zhang, L. Zhao, X. Lu, P. Zhang, S. He, G. Hu, X. Tang, Synthesis of a thiacalix [4] arenetetrasulfonate-functionalized reduced graphene oxide adsorbent for the removal of lead (II) and cadmium (II) from aqueous solutions, RSC Adv. 6 (2016) 113352–113365.

[38] T.S. Khokhar, F.N. Memon, S.S. Memon, A.A. Memon, A.A. Bhatti, S. Memon, Naringenin solubilizing and pH dependent releasing properties of water soluble p-sulphonatocalix [4] arene, Supramol. Chem. 33 (9) (2021) 493–503.

[39] S. Gul, F.N. Memon, S. Memon, Optimization of toxic metal adsorption on DEA-calix [4] arene appended silica resin using a central composite design, New J. Chem. 46 (2022) 3448–3463.

[40] K.H. Thebo, X. Qian, Q. Zhang, L. Chen, H.-M. Cheng, W. Ren, Highly stable graphene-oxide-based membranes with superior permeability, Nat. Commun. 9 (2018) 1–8.

[41] C. An, G. Huang, H. Yu, J. Wei, W. Chen, G. Li, Effect of short-chain organic acids and pH on the behaviors of pyrene in soil–water system, Chemosphere 81 (11) (2010) 1423–1429.

[42] X. Zou, H. Zhang, T. Chen, H. Li, C. Meng, J. Xia, J. Guo, Preparation and characterization of polyacrylamide/sodium alginate microspheres and its adsorption of MB dye, Colloids Surf. A Physicochem. Eng. Asp. 567 (2019) 184–192.

[43] A. Fakhri, S. Rashidi, M. Asif, A.A. Ibrahim, Synthesis and characterization of MnS2/reduced graphene oxide nanohybrid: an efficient adsorbent for pharmaceutical compound removal, Desalination Water Treat. 68 (2017) 236–244.

[44] N. Siva Kumar, A. Subba Reddy, V.M. Boddu, A. Krishnaiah, Development of chitosan-alginate based biosorbent for the removal of p-chlorophenol from aqueous medium, Toxicol. Environ. Chem. 91 (6) (2009) 1035–1054.

[45] H. Freundlich, W. Heller, The adsorption of cis-and trans-azobenzene, J. Am. Chem. Soc. 61 (8) (1939) 2228–2230.

[46] F.N. Memon, S. Memon, S. Memon, N. Memon, Synthesis and application of a new calix [4] arene based impregnated resin for the removal of endosulfan from an aqueous environment, J. Chem. Eng. Data 56 (8) (2011) 3336–3345.

[47] A.H. Alabi, A.I. Buhari-Alade, F.O. Sholaru, R.F. Awoyemi, Biosorption of phenols and dyes on Albizia lebbeck (Rattle seed) pod: equilibrium and kinetic studies, Int. J. Environ. Sci. 5 (2016) 154–165.

[48] M.O. Aremu, A. Alade, A. Bello, K. Salam, Kinetics and thermodynamics of 2, 4, 6–trichlorophenol adsorption onto activated carbon derived from flamboyant pod bark, Int. J. Environ. Appl. Sci. 13 (3) (2018) 158–166.

[49] A.M.d. Oliveira, M.A.L. Milhome, T.V. Carvalho, R.M. Cavalcante, R.F.d. Nascimento, Use of low-cost adsorbents to chlorophenols and organic matter removal of petrochemical wastewater, Orbital, Electron. J. Chem. 5 (2013) 171–178.

[50] M.A. Zazouli, D. Balarak, Y. Mahdavi, Application of Azolla for 2, 4, 6-Trichlorophenol (TCP) Removal from Aqueous Solutions, vol. 2, Archives of hygiene sciences, 2013, pp. 143–149.

[51] S. Ghezali, A. Mahdad-Benzerdjeb, M. Ameri, A.Z. Bouyakoub, Adsorption of 2, 4, 6-trichlorophenol on bentonite modified with benzyldimethyltetradecylammonium chloride, Chem. Int. 4 (2018) 24–32.

[52] M.K. Nazal, D. Gijjapu, N. Abuzaid, Study on adsorption performance of 2, 4, 6-trichlorophenol from aqueous solution onto biochar derived from macroalgae as an efficient adsorbent, Sep. Sci. & Techonol. 56 (21) (2021) 2183–2193.

[53] M.M. Motsa, J.M. Thwala, T.A. Msagati, B.B. Mamba, Adsorption of 2, 4, 6-trichlorophenol and ortho-nitrophenol from aqueous media using surfactant-modified clinoptilolite–polypropylene hollow fibre composites, Water Air Soil Pollut. 223 (2012) 1555–1569.

[54] B.I. Olu-Owolabi, A.H. Alabi, E.I. Unuabonah, P.N. Diagboya, L. Böhm, R.-A. Düring, Calcined biomass-modified bentonite clay for removal of aqueous metal ions, J. Environ. Chem. Eng. 4 (1) (2016) 1376–1382.

[55] N. Rahman, P. Varshney, Effective removal of doxycycline from aqueous solution using CuO nanoparticles decorated poly (2-acrylamido-2-methyl-1-propanesulfonic acid)/chitosan, Environ. Sci. Pollut. Res. 28 (2021) 43599–43617.

[56] A. Fakhri, S. Rashidi, M. Asif, A.A. Ibrahim, Microwave-assisted synthesis of SiC nanoparticles for the efficient adsorptive removal of nitroimidazole antibiotics from aqueous solution, Appl. Nanosci. 7 (2) (2017) 205.

[57] Y.-S. Ho, G. McKay, Pseudo-second order model for sorption processes, Process Biochem. 34 (5) (1999) 451–465.